Frontiers in Computing and Intelligent Systems
ISSN: 2832-6024 | Vol. 9, No. 1, 2024

A Delayed Mathematical Model of Population Pressure on the Atmospheric Level of Carbon Dioxide Gas

Tianchen Yao *

Faculty of Engineering, University of New South Wales, Sydney, 2050, Australia
* **Corresponding author Email**: yaotianchen639@163.com

Abstract: Effective control of carbon dioxide and methane emissions is the key to controlling global warming. For this reason, a delayed mathematical model of population pressure on the atmospheric level of carbon dioxide gas is put forward. The impact of the time lag on the model and exhibition of a Hopf bifurcation at the threshold of the time lag is analyzed in compliance with the allocation of the roots of the appropriate characteristic equation. Besides, the direction and stability of the Hopf bifurcation are determined by drawing support from the center manifold method. Eventually, computer numerical calculations are conducted to validate the correctness of our obtained analytical findings.

Keywords: Carbon Dioxide Gas; Delay; Hopf Bifurcation; Mathematical Model; Population Pressure.

1. Introduction

With the successive exploitation of science and technology industry, carbon dioxide emissions in the globe are also gradually increasing. With the successive expansion of carbon dioxide emissions, global warming has brought about the variability of the marine climate. Subsequently, many natural catastrophes arise, such as permanent glacier melting, sea level rising, frequent extreme weather and changes in ecosystem structure. In line with The Global Energy Review: Carbon Dioxide Emissions in 2021 released by The International Energy Agency (IEA), carbon dioxide emissions in the global energy sector exploded to 36.3 billion tons, increasing 6% year-on-year and exceeding the level before the outbreak of COVID-19 and setting a record [1]. Accordingly, in the context of tighter resource and environmental constraints, climate change caused by greenhouse gas emissions such as methane, nitrous oxide and ozone, especially carbon dioxide, has become the focus of attention of all sectors of the world [2].

In order to fight against the negative impacts caused by climate change, the world has made efforts to take various measures in all aspects. As early as May 9, 1992, the United Nations General Assembly adopted the Framework Convention on climate change. As of June 2016, 197 countries have adopted the Framework Convention on climate change, covering more than 65% of the total carbon emissions [3]. In 2015, the climate change conference held in Paris established a national independent contribution mechanism, requiring parties to refer to national conditions and propose emission reduction targets to address climate change in a "bottom-up" manner [4, 5]. After forwards, in 2019, the 49th plenary session of the Intergovernmental Panel on Climate Change (IPCC) adopted the improvement plan for the 2006 IPCC national inventory guidelines (IPCC, 2019), which clearly added the content of verifying the emission list based on atmospheric concentration and combined with the "top-down" (i.e. atmospheric inversion) method. In particular, the Chinese government has clearly put forward the carbon crest value by 2030 and the carbon neutralization target by 2060, from relative emission decline to absolute emission decline and zero emissions [6].

In recent years, some researchers have begun to study how to control carbon dioxide emissions from the perspective of system dynamics. Tennakone [7] revealed that severe deforestation could lead to a rapid increase of the carbon dioxide through constructing a biomass-carbon dioxide mathematical model and analyzing the stability of the constructed model. Alexiadis [8] explored the interplay between global warming and human activities with the help of control theory, and a feedback model is developed to analyze the impact of the carbon dioxide emission because of human activity on the global temperature. Subsequently, Dubey et al. [9] studied the connection between forestry resources and industrialization on account of population and population pressure by analyzing the dynamics of a nonlinear mathematical model. Then, Caetano et al. [10] presented some suggestions to cut down the carbon dioxide emissions with the aid of optimal control theory and by constructing a mathematical model. Misra and Verma [11] explored the influence of human population and forest biomass on carbon dioxide in the atmosphere through establishing a mathematical model. Sundar et al. [12] investigated the reduction of carbon dioxide by utilizing suitable absorbents around the source of carbon dioxide emission. Very recently, considering the interplay among carbon dioxide, human population, population pressure and forest biomass, Misra and Jha [13] formulated a mathematical model about population pressure on carbon dioxide as below on the foundation of the work by Misra and Verma [11]:

$$\begin{cases} \dfrac{dX(t)}{dt} = Q_0 + \lambda N(t) - \alpha X(t) - \lambda_1 X(t)F(t), \\ \dfrac{dN(t)}{dt} = sN(t)\left(1 - \dfrac{N(t)}{L}\right) - \theta X(t)N(t) + \iota\phi N(t)F(t), \\ \dfrac{dP(t)}{dt} = \theta_1 N(t) - \theta_0 P(t), \\ \dfrac{dF(t)}{dt} = \mu F(t)\left(1 - \dfrac{F(t)}{M}\right) - \phi N(t)F(t) - \phi_1 P(t)F^2(t). \end{cases} \tag{1}$$

Where, $X(t)$, $N(t)$, $P(t)$ and $F(t)$ denote the carbon dioxide consistence in the atmosphere, the human population, the population pressure and the forest biomass at

time t. Q_0 denotes the natural emission rate of carbon dioxide; λ denotes the anthropogenic emission rate coefficient of carbon dioxide; α is the natural depletion rate coefficient of carbon dioxide; λ_1 denotes the depletion rate coefficient of carbon dioxide due to forestry biomass; s and μ are the intrinsic growth rates of the human population and forest biomass, respectively; L and M are the carrying capacities of human population and forest biomass, respectively; θ denotes the reduction rate coefficient of the human population on account of adverse effects of carbon dioxide; θ_1 denotes the increasing rate coefficient of the population pressure due to the increase in the human population; θ_0 denotes the natural depletion rate coefficient of the population pressure; ϕ_1 denotes the diminution rate coefficient of the carrying capacity of forest biomass because of the population pressure; ϕ denotes the depletion rate coefficient of forest because of the human population; ι denotes the increasing rate coefficient of the human population because of forest biomass.

Obviously, the model (1) assumed that the growth of the human population gets favored by the forest biomass instantaneously. However, as is known to all that it is necessary to take some time to clear land for agriculture and roads etc. Additionally, in order to describe dynamics of mathematical models replying on the past history of the models, it is often needful to introduce time delays into the models [14-17]. Moreover, periodic solutions can appear due to the Hopf bifurcation in mathematical models with time delays [18-21]. Meng and Li [18] studied the bifurcating periodic solutions of a delayed phytoplankton-zooplankton system with Allee effect and linear harvesting. Bentout et al. [19] analyzed the Hopf bifurcation of a double age dependence epidemic model with two delays. Yang et al. [20] established a diffusive predator-prey model with time delay, and they revealed that time delay could make coexisting equilibrium lose stability and give rise to bifurcating periodic solution when it increases through a determinate threshold. Li et al. [21] delved into the Hopf bifurcation of a novel high-dimensional delayed fractional neural network model. Xu et al. [22] established a series of adequate conditions assuring the stability and the emergence of Hopf bifurcation for fractional-order competitive web site model of the Internet. There is also some work about Hopf bifurcation and periodic solutions in other fields [23-26]. Motivated by the work above and inspired by the fact that when the model (1) exhibits a Hopf bifurcation, the carbon dioxide concentration in the atmosphere will be out of control, we consider the model with a time lag as below:

$$\begin{cases} \dfrac{dX(t)}{dt} = Q_0 + \lambda N(t) - \alpha X(t) - \lambda_1 X(t)F(t), \\ \dfrac{dN(t)}{dt} = sN(t)\left(1 - \dfrac{N(t)}{L}\right) - \theta X(t)N(t) + \iota\phi N(t-\varsigma)F(t-\varsigma), \\ \dfrac{dP(t)}{dt} = \theta_1 N(t) - \theta_0 P(t), \\ \dfrac{dF(t)}{dt} = \mu F(t)\left(1 - \dfrac{F(t)}{M}\right) - \phi N(t-\varsigma)F(t-\varsigma) - \phi_1 P(t)F^2(t). \end{cases} \tag{2}$$

Where, ς is the time lag due to the interval that the growth of the human population needs to get favored by the forest biomass.

The remainder of the current paper is outlined as below. The impact of the time delay on the model and exhibition of Hopf bifurcation are explored in Section 2. Explicit formula direction and stability of the Hopf bifurcation are conducted in Section 3. Numerical simulating analysis is demonstrated in Section 4. A conclusion is drawn in Section 5.

2. Exhibition of Hopf Bifurcation

In the present section, we shall discuss the impact of the time lag on the model (2), and establish sufficient conditions for exhibition of Hopf bifurcation through analyzing allocation of the roots of the appropriate characteristic equation of the model (2). The method used in this section is common and simple, which is relatively intuitive.

If $s\alpha > \theta Q_0$ and $u > \dfrac{\phi L(s\alpha - \theta Q_0)}{s\alpha + \lambda\theta L}$, then the model (2) exhibits an interior equilibrium $U_*(X_*, N_*, P_*, F_*)$, where $X_* = \dfrac{Q_0 + \lambda N_*}{\alpha + \lambda_1 F_*}$, $P_* = A_1 N_*$, $N_* = \dfrac{B_2 F_*^2 + B_1 F_* + B_0}{C_1 F_* + C_0}$, and $A_1 = \dfrac{\theta_1}{\theta_0}$ and F_* is the positive root of Eq.(3) as below

$$f_3 F_*^3 + f_2 F_*^2 + f_1 F_* + f_0 = 0 \tag{3}$$

Where

$f_0 = \phi B_0 - uC_0$, $f_1 = \phi_1 A_1 B_0 + \phi B_1 + A_3 C_0 - uC_1$,
$f_2 = \phi_1 A_1 B_1 + \phi B_2 + A_3 C_1$, $f_3 = \phi_1 A_1 B_2$,
$B_0 = s\alpha - \theta Q_0$, $B_1 = \pi\phi\alpha + s\lambda_1$, $B_2 = \pi\phi\lambda_1$,
$C_0 = \alpha A_2 + \theta\lambda$, $C_1 = \lambda_1 A_2$, $A_2 = \dfrac{s}{L}$, $A_3 = \dfrac{u}{M}$.

The characteristic equation at $U_*(X_*, N_*, P_*, F_*)$ corresponding to the model (2) can be obtained as below

$$\begin{aligned} &\vartheta^4 + F_3\vartheta^3 + F_2\vartheta^2 + F_1\vartheta + F_0 \\ &\quad + (G_3\vartheta^3 + G_2\vartheta^2 + G_1\vartheta + G_0)e^{-\vartheta\varsigma} \\ &\quad + (H_2\vartheta^2 + H_1\vartheta + H_0)e^{-2\vartheta\varsigma} = 0, \end{aligned} \tag{4}$$

with

$F_0 = \theta_0 f_{44}(\lambda f_{21} - f_{11} f_{22}) + \theta_1 f_{14} f_{21} f_{43}$,
$F_1 = \theta_0(f_{11} f_{22} + f_{11} f_{44} + f_{22} f_{44}) - f_{11} f_{22} f_{44} - \lambda f_{21}(\theta_0 - f_{44})$,
$F_2 = f_{11} f_{22} + f_{11} f_{44} + f_{22} f_{44} - \theta_0(f_{11} + f_{22} + f_{44}) - \lambda f_{21}$,
$F_3 = \theta_0 - f_{11} - f_{22} - f_{44}$,
$G_1 = \theta_0 f_{21}(\lambda g_{44} - f_{14} g_{42}) - \theta_0 f_{11}(f_{22} g_{44} + f_{44} g_{22})$,
$G_1 = (\theta_0 - f_{11})(f_{22} g_{44} + f_{44} g_{22}) + \theta_0 f_{11}(g_{22} + g_{44})$,
$G_2 = f_{22} g_{44} + f_{44} g_{22} - (g_{22} + g_{44})(\theta_0 - f_{11})$,
$G_3 = -(g_{22} + g_{44})$, $H_0 = \theta_0 f_{11}(g_{24} g_{42} - g_{22} g_{44})$,
$H_1 = (\theta_0 - f_{11})(g_{22} g_{44} - g_{24} g_{42})$,
$H_2 = g_{22} g_{44} - g_{24} g_{42}$,

And

$f_{11} = -\alpha - \lambda_1 F_*$, $f_{14} = -\lambda_1 X_*$, $f_{21} = -\theta N_*$,

$f_{22}=s-\dfrac{2sN_*}{L}-\theta X_*$, $f_{43}=-2\phi_1 F_*$,

$f_{44}=u-\dfrac{2uF_*}{M}$, $g_{22}=\iota\phi F_*$, $g_{24}=\iota\phi N_*$,

$g_{42}=-\phi F_*$, $g_{44}=-\phi N_*$.

Multiplying by $e^{\vartheta\varsigma}$, Eq. (4) yields

$$\begin{aligned}&G_3\vartheta^3+G_2\vartheta^2+G_1\vartheta+G_0\\&\quad+(\vartheta^4+F_3\vartheta^3+F_2\vartheta^2+F_1\vartheta+F_0)e^{\vartheta\varsigma}\\&\quad+(H_2\vartheta^2+H_1\vartheta+H_0)e^{-\vartheta\varsigma}=0.\end{aligned}\tag{5}$$

For $\varsigma=0$, one has

$$\vartheta^4+J_3\vartheta^3+J_2\vartheta^2+J_1\vartheta+J_0=0\tag{6}$$

where

$J_0=G_0+F_0+H_0$, $J_1=G_1+F_1+H_1$,

$J_2=G_2+F_2+H_2$, $J_3=G_3+F_3$.

Lemma 1[13]. If $J_1(J_2J_3-J_1)>J_3^2J_0$, then the model (2) is locally asymptotically stable when $\varsigma=0$.

For $\varsigma>0$, putting $\vartheta=i\varpi$ ($\varpi>0$) into Eq. (5), then we get

$$\begin{cases}K_1(\varpi)\sin(\varsigma\varpi)+K_2(\varpi)\cos(\varsigma\varpi)=K_3(\varpi),\\K_4(\varpi)\cos(\varsigma\varpi)+K_5(\varpi)\sin(\varsigma\varpi)=K_6(\varpi),\end{cases}\tag{7}$$

with

$K_1(\varpi)=(H_1-F_1)\varpi+F_3\varpi^3$,

$K_2(\varpi)=\varpi^4-(H_2+F_2)\varpi^2+F_0+H_0$,

$K_3(\varpi)=G_2\varpi^2-G_0$,

$K_4(\varpi)=(H_1+F_1)\varpi-F_3\varpi^3$,

$K_5(\varpi)=\varpi^4+(H_2-F_2)\varpi^2+F_0-H_0$,

$K_6(\varpi)=G_3\varpi^3-G_1\varpi$.

Then, we obtain

$$\cos(\varsigma\varpi)=\frac{\Xi_1(\varpi)}{\Xi_0(\varpi)}\tag{8}$$

$$\sin(\varsigma\varpi)=\frac{\Xi_2(\varpi)}{\Xi_0(\varpi)}\tag{9}$$

where

$$\begin{aligned}\Xi_0(\varpi)&=\varpi^8+(F_3^2-2F_2)\varpi^6+(F_2^2+2F_0-H_2^2-2F_1F_3)\varpi^4\\&\quad+(F_1^2-2F_0F_2+2H_0H_2-H_1^2)\varpi^2+F_0^2-H_0^2,\\\Xi_1(\varpi)&=(G_2-G_3F_3)\varpi^6+(G_1F_3-G_2(F_2-H_2)-G_0-G_3(H_1-F_1))\varpi^4\\&\quad+(G_2(F_0-H_0)+G_0(F_2-H_2)+G_1(H_1-F_1))\varpi^2+G_0(F_0-H_0),\\\Xi_2(\varpi)&=G_3\varpi^7+(G_2F_3-G_1-G_3(F_2+H_2))\varpi^5\\&\quad+(G_1(F_2+H_2)-G_3(F_0+H_0)-G_2(H_1+F_1)-G_0F_3)\varpi^3\\&\quad+(G_0(F_1+H_1)-G_1(H_0+F_0))\varpi.\end{aligned}$$

Further, the algebraic equation regarding ϖ can be get

$$\Xi_0^2(\varpi)-\Xi_1^2(\varpi)-\Xi_2^2(\varpi)=0.\tag{10}$$

Clearly, one can get all the roots of Eq. (10) once the parameters of the model (2) are determined. Thus, we suppose that Eq. (10) has positive root ϖ_0. Then Eq. (5) has roots $\pm i\varpi_0$. For ϖ_0, on the foundation of Eq. (8), one has

$$\varsigma^i=\frac{1}{\varpi_0}\times\arccos\left[\frac{\Xi_1(\varpi_0)}{\Xi_0(\varpi_0)}\right]+\frac{2i\pi}{\varpi_0},\ i=0,1,2,\cdots.\tag{11}$$

Denote

$$\varsigma_0=\min\{\varsigma^i\},\ i=0,1,2,\cdots.\tag{12}$$

Differentiating Eq.(6) about ς, then

$$\left[\frac{d\vartheta}{d\varsigma}\right]^{-1}=-\frac{\Xi_4(\vartheta)}{\Xi_3(\vartheta)}-\frac{\varsigma}{\vartheta}\tag{13}$$

with

$\Xi_3(\vartheta)=(\vartheta^5+F_3\vartheta^4+F_2\vartheta^3+F_1\vartheta^2+F_0\vartheta)e^{\vartheta\varsigma}-(H_2\vartheta^3+H_1\vartheta^2+H_0\vartheta)e^{-\vartheta\varsigma}$

, $\Xi_4(\vartheta)=3G_3\vartheta^2+2G_2\vartheta+G_1+(4\vartheta^3+3F_3\vartheta^2+2F_2\vartheta+F_1)e^{\vartheta\varsigma}+(2H_2\vartheta+H_1)e^{-\vartheta\varsigma}$.

Then

$$\mathrm{Re}\left[\frac{d\vartheta}{d\varsigma}\right]^{-1}_{\vartheta=i\varpi_0}=\frac{\Xi_4^*(\varpi_0)}{\Xi_3^*(\varpi_0)}\tag{14}$$

Where

$$\begin{aligned}\Xi_3^*(\varpi_0)&=((\varpi_0^5-(F_2+H_2)\varpi_0^3+(F_0+H_0)\varpi_0)\sin\varpi_0\varsigma_0\\&\quad+((F_1-H_1)\varpi_0^2-F_3\varpi_0^4)\cos\varpi_0\varsigma_0)^2\\&\quad+(((F_2-H_2)\varpi_0^3-\varpi_0^5+(F_0+H_0)\varpi_0)\cos\varpi_0\varsigma_0\\&\quad+((F_1+H_1)\varpi_0^2-F_3\varpi_0^4)\sin\varpi_0\varsigma_0)^2,\\\Xi_4^*(\varpi_0)&=((\varpi_0^5-(F_2+H_2)\varpi_0^3+(F_0+H_0)\varpi_0)\sin\varpi_0\varsigma_0\\&\quad+((F_1-H_1)\varpi_0^2-F_3\varpi_0^4)\cos\varpi_0\varsigma_0)\\&\quad\times(G_1-3G_3\varpi_0^2+(F_1+H_1-3F_3\varpi_0^2)\cos\varpi_0\varsigma_0\\&\quad-((2F_2-2H_2)\varpi_0-4\varpi_0^3)\sin\varpi_0\varsigma_0)\\&\quad+(((F_2-H_2)\varpi_0^3-\varpi_0^5+(H_0+F_0)\varpi_0)\cos\varpi_0\varsigma_0\\&\quad+((F_1+H_1)\varpi_0^2-\varpi_0^4)\sin\varpi_0\varsigma_0)\\&\quad\times(2G_2\varpi_0+(F_1-H_1-3F_3\varpi_0^2)\sin\varpi_0\varsigma_0\\&\quad+((2F_2+2H_2)\varpi_0-4\varpi_0^3)\cos\varpi_0\varsigma_0).\end{aligned}$$

Apparently, if $\Xi_4^*(\varpi_0)\neq 0$ then we have $\mathrm{Re}\left[d\vartheta/d\varsigma\right]^{-1}_{\vartheta=i\varpi_0}\neq 0$. On the foundation of the Hop bifurcation theorem in [27], one can get the results as below.

Theorem 1. If $s\alpha>\theta Q_0$ and $u>\dfrac{\phi L(s\alpha-\theta Q_0)}{s\alpha+\lambda\theta L}$, then the interior equilibrium $U_*(X_*,N_*,P_*,F_*)$ is locally asymptotically stable whenever $\varsigma\in[0,\varsigma_0)$; while a Hopf bifurcation emerges near the interior equilibrium $U_*(X_*,N_*,P_*,F_*)$ when $\varsigma=\varsigma_0$ and a family of periodic solutions bifurcate from the interior equilibrium $U_*(X_*,N_*,P_*,F_*)$.

3. Direction and Stability of the Periodic Solutions

In the current section, we will deduce explicit formulas which can determine the direction and stability of the periodic solutions by using the center manifold method innovated by Hassardet al [27]. The calculation steps of the method we used are complicated. Nevertheless, the results we obtained can determine the direction and stability of the periodic solutions with the6parameters of the model (2) obviously. Define $C=C([-1,0],\mathrm{R}^4)$, $\varsigma=\varsigma_0+j$ and $j\in\mathrm{R}$. Setting $v_1(t)=X(t)-X_*$, $v_2(t)=N(t)-N_*$, $v_3(t)=P(t)-P_*$, $v_4(t)=F(t)-F_*$ and $t\to(t/\varsigma)$. Then the model (2) equals

$$\dot{v}(t)=L_j(v_t)+F(j,v_t) \tag{15}$$

Where $L_j:C\to\mathrm{R}^4$ and $F:\mathrm{R}\times C\to\mathrm{R}^4$ are presented by

$$L_j(\psi)=(\varsigma_0+j)[L_1\psi(0)+L_2\psi(-1)] \tag{16}$$

with

$$L_1=\begin{pmatrix} f_{11} & \lambda & 0 & f_{14}\\ f_{21} & f_{22} & 0 & 0\\ 0 & \theta_1 & -\theta_0 & 0\\ 0 & 0 & f_{43} & f_{44}\end{pmatrix},$$

$$L_2=\begin{pmatrix} 0 & \lambda & 0 & 0\\ 0 & g_{22} & 0 & g_{24}\\ 0 & 0 & 0 & 0\\ 0 & g_{42} & 0 & g_{44}\end{pmatrix},$$

and

$$F(j,\psi)=(\varsigma_0+j)(F_1,F_2,0,F_4)^T \tag{17}$$

where

$F_1=-\lambda\psi_1(0)\psi_4(0)$,

$F_2=-\dfrac{s}{L}\psi_2^2(0)-\theta\psi_1(0)\psi_2(0)+\iota\phi\psi_2(-1)\psi_4(-1)$,

$F_4=-2\phi_1F_*\psi_3(0)\psi_4(0)-\left(\dfrac{u}{M}+\phi_1P_*\right)\psi_4^2(0)-\phi_1\psi_3(0)\psi_4^2(0)+\phi\psi_2(-1)\psi_4(-1)$

On the foundation of the Riesz representation theorem, one can get $\eta(\kappa,j)$ for $\kappa\in[-1,0]$ satisfying

$$L_j(\psi)=\int_{-1}^{0}d\eta(\kappa,j)\psi(\kappa),\ \kappa\in C([-1,0],\mathrm{R}^4). \tag{18}$$

Setting

$$\eta(\kappa,j)=(\varsigma_0+j)(L_1\Upsilon(\kappa)+L_2\Upsilon(\kappa+1)), \tag{19}$$

and $\Upsilon(\kappa)$ is Dirac delta function. For $\kappa\in C([-1,0],\mathrm{R}^4)$, define

$$D(j)\psi(\kappa)=\begin{cases}\dfrac{d\psi(\kappa)}{d\kappa}, & -1\le\kappa<0,\\ \int_{-1}^{0}d\eta(\kappa,j)\psi(s), & \kappa=0,\end{cases} \tag{20}$$

and

$$R(j)\psi(\kappa)=\begin{cases}0, & -1\le\kappa<0,\\ F(j,\psi), & \kappa=0.\end{cases} \tag{21}$$

Thus, system (15) becomes

$$\dot{v}(t)=A(j)v_t+R(j)v_t. \tag{22}$$

For $\varphi\in C^1([0,1],(\mathrm{R}^4)^*)$, define

$$D^*(j)\varphi(s)=\begin{cases}\dfrac{d\varphi(s)}{ds}, & 0<s\le 1,\\ \int_{-1}^{0}d\eta^T(s,0)\varphi(-s), & s=0,\end{cases} \tag{23}$$

and

$$\left\langle\varphi(s),\psi(\kappa)\right\rangle=\bar{\varphi}(0)\psi(0)-\int_{\kappa=-1}^{0}\int_{\xi=0}^{\kappa}\bar{\varphi}(\xi-\kappa)d\eta(\kappa)\psi(\xi)d\xi \tag{24}$$

Let $\Theta(\kappa)=(1,\Theta_2,\Theta_3,\Theta_4)^Te^{i\varsigma_0\varpi_0\kappa}$ is the eigenvector of $D(0)$ belonged to $+i\varpi_0\varsigma_0$ and $\Theta^*(s)=Q(1,\Theta_2^*,\Theta_3^*,\Theta_4^4)^Te^{i\varsigma_0\varpi_0 s}$ s the eigenvector of $D^*(0)$ belonged to $-i\varpi_0\varsigma_0$. Correspondingly, in view of the definitions of $D(0)$) and $D^*(0)$, we can obtain

$$\Theta_2=\frac{f_{14}f_{21}+g_{24}e^{-i\varsigma_0\varpi_0}(i\varpi_0-f_{11})}{\lambda g_{24}e^{-i\varsigma_0\varpi_0}+f_{21}(i\varpi_0-f_{22}-g_{22}e^{-i\varsigma_0\varpi_0})}$$

$$\Theta_3=\frac{\theta_1\Theta_2}{i\varpi_0+\theta_0},\ \Theta_4=\frac{i\varpi_0-f_{11}-\lambda g_{22}}{f_{14}},$$

$$\Theta_2^*=-\frac{i\varpi_0+f_{11}}{f_{21}},\quad \Theta_3^*=\frac{f_{43}\Theta_4^*}{\theta_0-i\varpi_0},$$

$$\Theta_4^4=-\frac{f_{14}+g_{24}e^{i\varsigma_0\varpi_0}}{i\varpi_0+f_{44}+g_{44}e^{i\varsigma_0\varpi_0}}.$$

From Eq. (24), one has

$$\bar{Q}=[1+\Theta_2\bar{\Theta}_2^*+\Theta_3\bar{\Theta}_3^*+\Theta_4\bar{\Theta}_4^* + \varsigma_0 e^{-i\varsigma_0\varpi_0}(\Theta_2(g_{22}\bar{\Theta}_2^*+g_{42}\bar{\Theta}_4^*) + \Theta_4(g_{24}\bar{\Theta}_2^*+g_{44}\bar{\Theta}_4^*))]^{-1},$$

such that $\langle\Theta^*,\Theta\rangle=1$ and $\langle\Theta^*,\bar{\Theta}\rangle=0$.

Then, we can acquire the explicit expressions of h_{20}, h_{11}, h_{02} and h_{21} based on the method used in [28, 29]:

$$h_{20}=2\varsigma_0\bar{Q}(h_{201}+\bar{\Theta}_2^*h_{202}+\bar{\Theta}_4^*h_{204}),$$
$$h_{11}=\varsigma_0\bar{Q}(h_{111}+\bar{\Theta}_2^*h_{112}+\bar{\Theta}_4^*h_{114}),$$
$$h_{02}=2\varsigma_0\bar{Q}(h_{021}+\bar{\Theta}_2^*h_{022}+\bar{\Theta}_4^*h_{024}),$$
$$h_{21}=2\varsigma_0\bar{Q}(h_{211}+\bar{\Theta}_2^*h_{212}+\bar{\Theta}_4^*h_{214}),$$

with

$$h_{201}=-\lambda\Theta_4,$$

$$h_{202}=-\frac{s}{L}\Theta_2^2-\theta\Theta_2+\iota\phi\Theta_2\Theta_4e^{-2i\varsigma_0\varpi_0},$$

$$h_{204}=-2\phi_1F_*\Theta_3\Theta_4-\left(\frac{u}{M}+\phi_1P_*\right)\Theta_4^2-\phi\Theta_2\Theta_4e^{-2i\varsigma_0\varpi_0},$$

$$h_{111}=-\lambda(\bar{\Theta}_4+\Theta_4),$$

$$h_{112}=-\frac{2s}{L}\Theta_2\bar{\Theta}_2-\theta(\bar{\Theta}_2+\Theta_2)+\iota\phi(\Theta_2\bar{\Theta}_4+\bar{\Theta}_2\Theta_4),$$

$$h_{114}=-2\phi_1F_*(\Theta_3\bar{\Theta}_4+\bar{\Theta}_3\Theta_4)-2\left(\frac{u}{M}+\phi_1P_*\right)\Theta_4\bar{\Theta}_4-\phi(\Theta_2\bar{\Theta}_4+\bar{\Theta}_2\Theta_4),$$

$$h_{021}=-\lambda\bar{\Theta}_4,$$

$$h_{022}=-\frac{s}{L}\bar{\Theta}_2^2-\theta\bar{\Theta}_2+\iota\phi\bar{\Theta}_2\bar{\Theta}_4e^{2i\varsigma_0\varpi_0},$$

$$h_{024}=-2\phi_1F_*\bar{\Theta}_3\bar{\Theta}_4-\left(\frac{u}{M}+\phi_1P_*\right)\bar{\Theta}_4^2-\phi\bar{\Theta}_2\bar{\Theta}_4e^{2i\varsigma_0\varpi_0},$$

$$h_{211}=-\lambda\left(W_{11}^{(1)}(0)\Theta_4+\frac{1}{2}W_{20}^{(1)}(0)\bar{\Theta}_4+W_{11}^{(4)}(0)+\frac{1}{2}W_{20}^{(4)}(0)\right),$$

$$h_{212}=-\frac{s}{L}(2W_{11}^{(2)}(0)\Theta_2+W_{20}^{(2)}(0)\bar{\Theta}_2) -\theta\left(W_{11}^{(2)}(0)\Theta_2+\frac{1}{2}W_{20}^{(2)}(0)\bar{\Theta}_2+W_{11}^{(2)}(0)+\frac{1}{2}W_{20}^{(2)}(0)\right) +\iota\phi\left(W_{11}^{(2)}(-1)\Theta_4e^{-i\varsigma_0\varpi_0}+\frac{1}{2}W_{20}^{(2)}(-1)\bar{\Theta}_4e^{i\varsigma_0\varpi_0}\right) +\iota\phi\left(W_{11}^{(4)}(-1)\Theta_2e^{-i\varsigma_0\varpi_0}+\frac{1}{2}W_{20}^{(4)}(-1)\bar{\Theta}_2e^{i\varsigma_0\varpi_0}\right),$$

$$h_{214}=-2\phi_1F_*\left(W_{11}^{(3)}(0)\Theta_4+\frac{1}{2}W_{20}^{(3)}(0)\bar{\Theta}_4+W_{11}^{(4)}(0)\Theta_3+\frac{1}{2}W_{20}^{(4)}(0)\bar{\Theta}_3\right) -\left(\frac{u}{M}+\phi_1P_*\right)\left(2W_{11}^{(4)}(0)\Theta_4+W_{20}^{(4)}(0)\bar{\Theta}_4\right)-\phi_1(\bar{\Theta}_3\Theta_4^2+2\Theta_3\Theta_4\bar{\Theta}_4) -\phi\left(W_{11}^{(2)}(-1)\Theta_4e^{-i\varsigma_0\varpi_0}+\frac{1}{2}W_{20}^{(2)}(-1)\bar{\Theta}_4e^{i\varsigma_0\varpi_0}\right) -\phi\left(W_{11}^{(4)}(-1)\Theta_2e^{-i\varsigma_0\varpi_0}+\frac{1}{2}W_{20}^{(4)}(-1)\bar{\Theta}_2e^{i\varsigma_0\varpi_0}\right),$$

with

$$W_{20}(\kappa)=\frac{ih_{20}}{\varsigma_0\varpi_0}\Theta(0)+\frac{i\bar{h}_{02}}{3\varsigma_0\varpi_0}\bar{\Theta}(0)+\Upsilon_1e^{2i\varsigma_0\varpi_0\kappa}, \quad (25)$$

$$W_{11}(\kappa)=-\frac{ih_{11}}{\varsigma_0\varpi_0}\Theta(0)+\frac{i\bar{h}_{11}}{\varsigma_0\varpi_0}\bar{\Theta}(0)+\Upsilon_2, \quad (26)$$

and $\Upsilon_1=(\Upsilon_{11},\Upsilon_{12},\Upsilon_{13},\Upsilon_{14})^T\in\mathrm{R}^4$ and $\Upsilon_2=(\Upsilon_{21},\Upsilon_{22},\Upsilon_{23},\Upsilon_{24})^T\in\mathrm{R}^4$ are denoted as below:

$$\Upsilon_{11}=\frac{2}{\Upsilon_{20}}\begin{vmatrix} h_{201} & \lambda & 0 & f_{14}\\ h_{202} & 2i\varpi_0-f_{22}-g_{22}e^{-2i\varsigma_0\varpi_0} & 0 & -g_{24}e^{-2i\varsigma_0\varpi_0}\\ 0 & -\theta_1 & 2i\varpi_0+\theta_0 & 0\\ h_{204} & -g_{42}e^{-2i\varsigma_0\varpi_0} & -f_{43} & 2i\varpi_0-g_{44}e^{-2i\varsigma_0\varpi_0}\end{vmatrix},$$

$$\Upsilon_{12}=\frac{2}{\Upsilon_{20}}\begin{vmatrix} 2i\varpi_0-f_{11} & h_{201} & 0 & f_{14}\\ f_{21} & h_{202} & 0 & -g_{24}e^{-2i\varsigma_0\varpi_0}\\ 0 & 0 & 2i\varpi_0+\theta_0 & 0\\ 0 & h_{204} & -f_{43} & 2i\varpi_0-g_{44}e^{-2i\varsigma_0\varpi_0}\end{vmatrix},$$

$$\Upsilon_{13}=\frac{2}{\Upsilon_{20}}\begin{vmatrix} 2i\varpi_0-f_{11} & \lambda & h_{201} & f_{14}\\ f_{21} & 2i\varpi_0-f_{22}-g_{22}e^{-2i\varsigma_0\varpi_0} & h_{202} & -g_{24}e^{-2i\varsigma_0\varpi_0}\\ 0 & -\theta_1 & 0 & 0\\ 0 & -g_{42}e^{-2i\varsigma_0\varpi_0} & h_{204} & 2i\varpi_0-g_{44}e^{-2i\varsigma_0\varpi_0}\end{vmatrix},$$

$$\Upsilon_{14}=\frac{2}{\Upsilon_{20}}\begin{vmatrix} 2i\varpi_0-f_{11} & \lambda & 0 & h_{201}\\ f_{21} & 2i\varpi_0-f_{22}-g_{22}e^{-2i\varsigma_0\varpi_0} & 2i\varpi_0+\theta_0 & h_{202}\\ 0 & -\theta_1 & 0 & 0\\ 0 & -g_{42}e^{-2i\varsigma_0\varpi_0} & -f_{43} & h_{204}\end{vmatrix},$$

$$\Upsilon_{21}=-\frac{2}{\Upsilon_{11}}\begin{vmatrix} h_{111} & \lambda & 0 & f_{14} \\ h_{112} & f_{22}+g_{22} & 0 & g_{24} \\ 0 & \theta_1 & -\theta_0 & 0 \\ h_{114} & g_{42} & f_{43} & f_{44}+g_{44} \end{vmatrix},$$

$$\Upsilon_{22}=-\frac{2}{\Upsilon_{11}}\begin{vmatrix} f_{11} & h_{111} & 0 & f_{14} \\ f_{21} & h_{112} & 0 & g_{24} \\ 0 & 0 & -\theta_0 & 0 \\ 0 & h_{114} & f_{43} & f_{44}+g_{44} \end{vmatrix},$$

$$\Upsilon_{23}=-\frac{2}{\Upsilon_{11}}\begin{vmatrix} f_{11} & \lambda & h_{111} & f_{14} \\ f_{21} & f_{22}+g_{22} & h_{112} & g_{24} \\ 0 & \theta_1 & 0 & 0 \\ 0 & g_{42} & h_{114} & f_{44}+g_{44} \end{vmatrix},$$

$$\Upsilon_{24}=-\frac{2}{\Upsilon_{11}}\begin{vmatrix} f_{11} & \lambda & 0 & h_{111} \\ f_{21} & f_{22}+g_{22} & 0 & h_{112} \\ 0 & \theta_1 & -\theta_0 & 0 \\ 0 & g_{42} & f_{43} & h_{114} \end{vmatrix},$$

with

$$\Upsilon_{20}=\begin{vmatrix} 2i\varpi_0-f_{11} & \lambda & 0 & f_{14} \\ f_{21} & 2i\varpi_0-f_{22}-g_{22}e^{-2i\varsigma_0\varpi_0} & 0 & -g_{24}e^{-2i\varsigma_0\varpi_0} \\ 0 & -\theta_1 & 2i\varpi_0+\theta_0 & 0 \\ 0 & -g_{42}e^{-2i\varsigma_0\varpi_0} & -f_{43} & 2i\varpi_0-g_{44}e^{-2i\varsigma_0\varpi_0} \end{vmatrix},$$

$$\Upsilon_{11}=\begin{vmatrix} f_{11} & \lambda & 0 & f_{14} \\ f_{21} & f_{22}+g_{22} & 0 & g_{24} \\ 0 & \theta_1 & -\theta_0 & 0 \\ 0 & g_{42} & f_{43} & f_{44}+g_{44} \end{vmatrix}.$$

Accordingly, we have

$$C_1(0)=\frac{i}{2\varpi_0\varsigma_0}\left(h11h20-2\,|\,h_{11}\,|^2-\frac{|\,h_{02}\,|^2}{3}\right)+\frac{h_{21}}{2},$$

$$\Delta_1=-\frac{\mathrm{Re}\{C_1(0)\}}{\mathrm{Re}\{\vartheta'(\varsigma_0)\}},$$

$$\Delta_2=2\,\mathrm{Re}\{C_1(0)\}.$$

Conclusively, we can acquire the theorem depicting properties of the Hopf bifurcation at $\varsigma=\varsigma_0$ stated as below.

Theorem 2. Supposing that $\Delta_1>0$ ($\Delta_1<0$), then Hopf bifurcation emerging at $\varsigma=\varsigma_0$ is supercritical (subscriptical); supposing that $\Delta_2>0$ ($\Delta_2<0$), then the periodic solutions bifurcating from the interior equilibrium $U_*(X_*,N_*,P_*,F_*)$ are stable (unstable).

4. Numerical Simulations

In the current section, we will execute some numerical calculations to validate the effectiveness of obtained theoretical results by using MATLAB software package 7.0 and the same method used in [28]. We choose some same values of parameters in the model (1) by Misra and Jha [13], and give attention to the sufficient requirements for the emergence of Hopf bifurcation in the present paper. Setting $Q_0=1$, $\lambda=0.05$, $\alpha=0.003$, $\lambda_1=0.0001$, $s=0.01$, $L=1000$, $\theta=0.00001$, $\iota=0.077$, $\phi=0.0002$, $\theta_1=0.0002$, $\theta_0=0.005$, $u=0.2$, $M=2000$, $\varphi_1=0.00002$, the model (2) equals:

$$\begin{cases} \dfrac{dX(t)}{dt}=1+0.05N(t)-0.003X(t)-0.0001X(t)F(t), \\ \dfrac{dN(t)}{dt}=0.01N(t)\left(1-\dfrac{N(t)}{1000}\right)-0.00001X(t)N(t)+0.0000154N(t-\varsigma)F(t-\varsigma), \\ \dfrac{dP(t)}{dt}=0.0002N(t)-0.005P(t), \\ \dfrac{dF(t)}{dt}=0.2F(t)\left(1-\dfrac{F(t)}{2000}\right)-0.0002N(t-\varsigma)F(t-\varsigma)-0.00002P(t)F^2(t). \end{cases} \tag{27}$$

Evidently, $s\alpha=0.00003>\theta Q_0=0.00001$ and $u=0.2>\dfrac{\phi L(s\alpha-\theta Q_0)}{s\alpha+\lambda\theta L}=0.0075$. Conclusively, the

conditions for the exhibition of an interior equilibrium of the model (28) hold. Further, With the aid of MATLAB software package, we get the unique interior equilibrium $U_*(903.4307, 456.4565, 18.2583, 233.6929)$. Correspondingly, in line with Lemma 1, the model (28) is locally asymptotically steady when $\varsigma = 0$.

For $\varsigma > 0$, by some calculations, we obtain $\varpi_0 = 3.2683$, $\varsigma_0 = 20.0629$ and $\vartheta'(\varsigma_0) = -3.9658e-004 + i1.6086e-005$. Accordingly, adequate conditions for the exhibition of Hopf bifurcation are satisfied. Setting $\varsigma = 19.5945 \in [0, \varsigma_0)$, as can be seen from Figure 1 that the values of the four states in the model (28) tend to the interior equilibrium $U_*(903.4307, 456.4565, 18.2583, 233.6929)$ gradually. This suggests that the model (28) is locally asymptotically steady, which can be also described by Figure 2. Next, we fix $\varsigma = 21.3107 > \varsigma_0$. In this case, the model (28) is bereft of its stability and a Hopf bifurcation emerges near $\varsigma_0 = 20.0629$, and a cluster of periodic solutions occur around $U_*(903.4307, 456.4565, 18.2583, 233.6929)$. As shown in Figure 3, the values of the four states in the model (28) exhibit periodic oscillations near the interior equilibrium $U_*(903.4307, 456.4565, 18.2583, 233.6929)$. This phenomenon can be also described in Figure 4. These results are consistent with the Theorem 1.

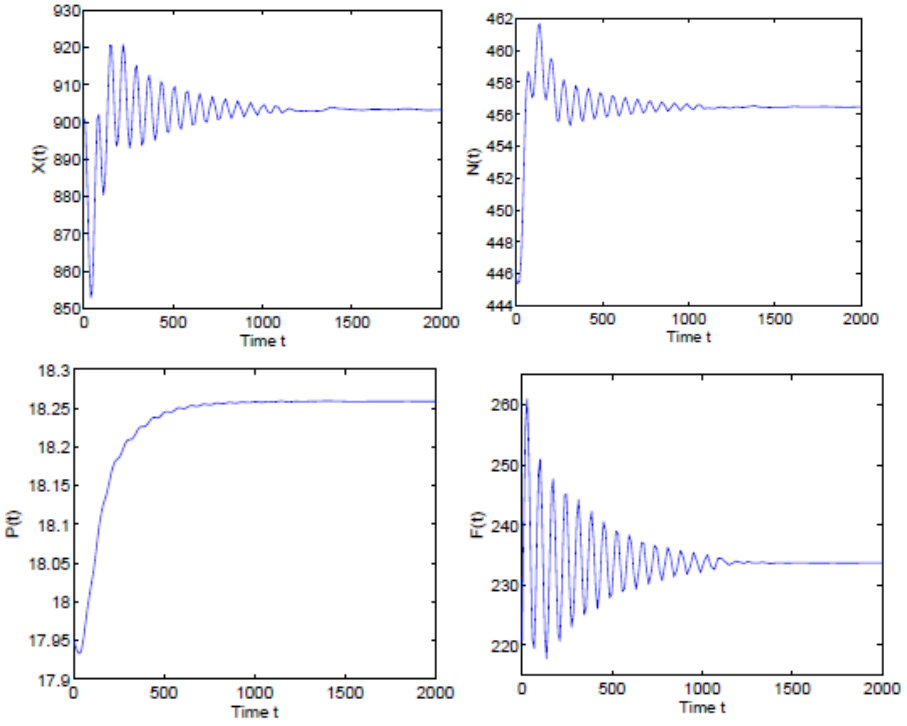

Figure 1. Time plots of the model (28) for $\varsigma = 19.5945 < \varsigma_0$

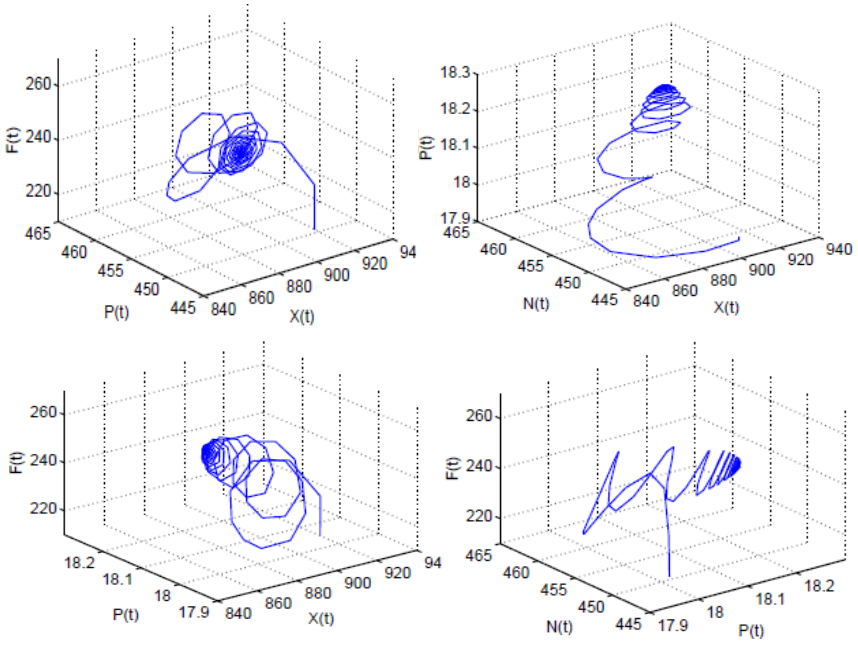

Figure 2. Phase plots of the model (28) for $\varsigma = 19.5945 < \varsigma_0$

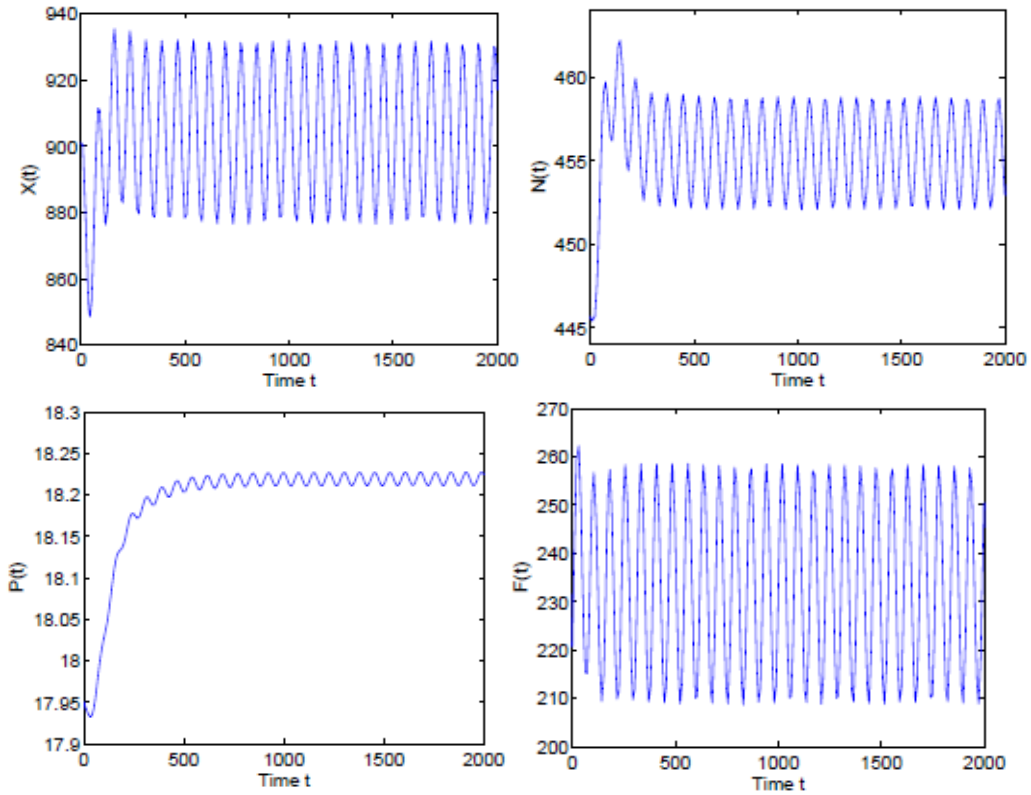

Figure 3. Time plots of the model (28) for $\varsigma = 21.3107 > \varsigma_0$

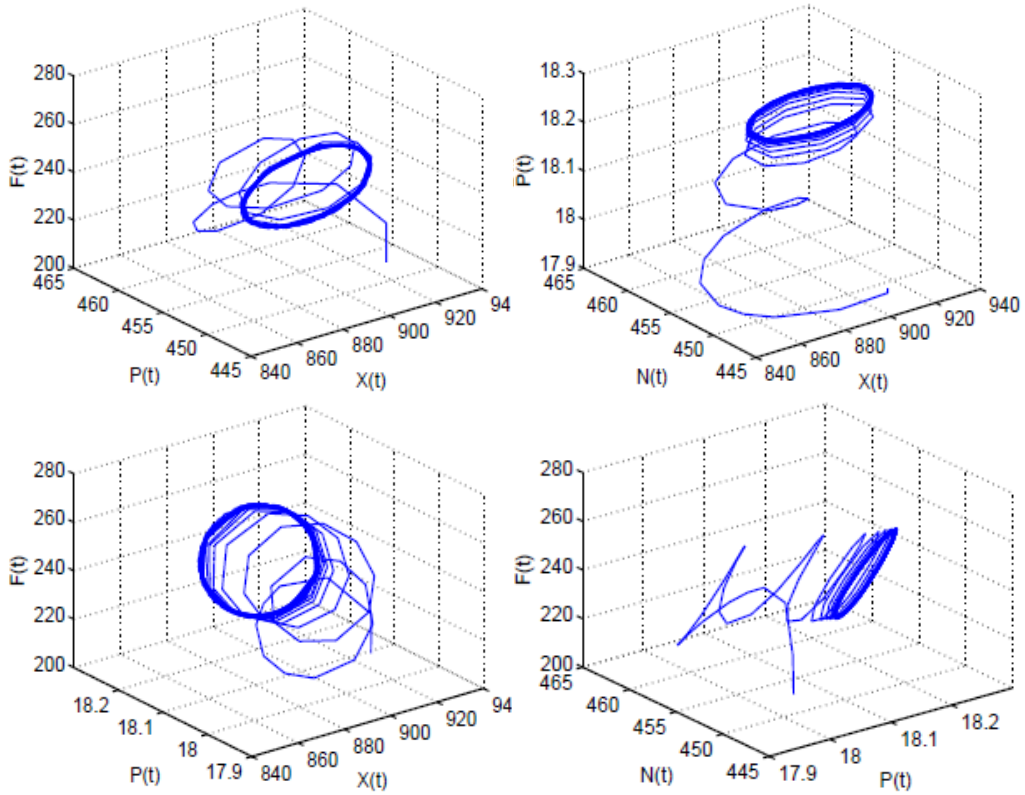

Figure 4. Phase plots of the model (28) for $\varsigma = 21.3107 > \varsigma_0$

5. Conclusion

In the current paper, a delayed mathematical model of population pressure on the atmospheric level of carbon dioxide gas is proposed by introducing the time delay on account of the interval that the growth of the human population needs to get favored by the forest biomass into the model innovated by Misra and Jha. The main aim of the current paper is to analyze the impact of the time delay on our proposed model. A sequence of adequate criteria for the local stability of the model and emergence of Hopf bifurcation are derived with the help of the eigenvalue method. Direction and stability of the Hopf bifurcation are probed by utilizing the center manifold method. We find that when the value of the

time delay on account of the interval that the growth of the human population needs to get favored by the forest biomass is suitable small ($\varsigma \in [0, \varsigma_0)$), the model is locally asymptotically steady. Under such circumstances, the carbon dioxide consistence in the atmosphere, the human population, the population pressure and the forest biomass gradually tend to interior equilibrium $U_*(X_*, N_*, P_*, F_*)$, and the carbon dioxide consistence in the atmosphere can be predicted and controlled. Otherwise, once the value of the time delay on account of the interval that the growth of the human population needs to get favored by the forest biomass exceeds the threshold ς_0, then the model loses its stability and the carbon dioxide consistence in the atmosphere, the human population, the population pressure and the forest biomass tend to periodic oscillation, and the carbon dioxide consistence in the atmosphere will be out of control. In this perspective, it is suggested that human beings should make rational use of forest resources and avoid excessive deforestation to maintain ecological balance.

References

[1] https://www.huaon.com/channel/trend/799762.html, accessed on June 29, 2022.

[2] Y. X. Liu, Y. Zhang, Z. Li, H. C. Guo, Research status analysis of global greenhouse gas emission based on bibliometrics (in Chinese), Acta Scientiae Circumstantiae, 41(2021): 4740-4751.

[3] P. M. Cox, R. Betts, C. D. Jones, S. A. Spall, I. J. Totterdell, Acceleration of global warming due to carbon-cycle feedbacks in a coupled climate model, Nature, 408(2000): 184-187.

[4] Y. Liu, J. Wang, K. Che, Z. N. Cai, D. X. Yang, L. Wu, Satellite remote sensing of greenhouse gases: Progress and trends (in Chinese), National Remote Sensing Bulletin, 25(2021): 53-64.

[5] Y. D. Chen, W. J. Cai, C. Wang, The characteristics of Intended Nationally Determined Contributions (in Chinese), Climate Change Research, 14(2018): 295-302.

[6] http://www.acet-ceca.com/desc/10739.html, accessed on July 3, 2022.

[7] K. Tennakone, Stability of the biomass-carbon dioxide equilibrium in the atmosphere: mathematical model, Applied Mathematics and Computation, 35(1990): 125-130.

[8] A. Alexiadis, Global warming and human activity: A model for studying the potential instability of the carbon dioxide/ temperature feedback mechanism, Ecology Modelling, 203 (2007): 243-256.

[9] B. Dubey, S. Sharma, P. Sinha, J. B. Shukla, Modelling the depletion of forestry resources by population and population pressure augmented industrialization, Appl. Math. Model, 33(2009): 3002-3014.

[10] M. A. L. Caetano, D. F. M. Gherardi, T. Yoneyama, An optimized policy for the reduction of CO2 emission in the Brazilian Legal Amazon, Ecology Modelling, 222(2011): 2835-2840.

[11] A. K. Misra, M. Verma, A mathematical model to study the dynamics of carbon dioxidegas in the atmosphere, Applied Mathematics and Computation, 219(2013): 8595-8609.

[12] S. Sundar, R. Naresh, A. K. Misra, A. Tripathi, Modeling the dynamics of carbon dioxide removal in the atmosphere, Computational Ecology Software, 4(2014): 248-268.

[13] A. K. Misra, A. Jha, Modelling the effect of population pressure on the dynamics of carbon dioxide gas, Journal of Applied Mathematics and Computing, 67(2021): 623-640.

[14] J. F. Zhang, Bifurcation analysis of a modified Holling-Tanner predator-prey modelwith time delay, Applied Mathematical Modelling, 36(2012): 1219-1231.

[15] Z. Z. Zhang, G. U. Rahman, J. F. Gomez-Aguilar, J. Torres-Jimenez, Dynamical aspects of a delayed epidemic model with subdivision of susceptible population and control strategies, Chaos, Solitons and Fractals, 160(2022):112194.

[16] J. N. Wang, H. B. Shi, L. Xu, L. Zhang, Hopf bifurcation and chaos of tumor-Lymphatic model with two time delays, Chaos, Solitons and Fractals, 157(2022):111922.

[17] N. Keshri, B. K. Mishra, Two time-delay dynamic model on the transmissionof malicious signals in wireless sensor network, Chaos, Solitons and Fractals, 68 (11) (2014): 151-158.

[18] X. Y. Meng, J. Li, Stability and Hopf bifurcation analysis of a delayed phytoplankton-zooplankton model with Allee effect and linear harvesting, Mathematical Biosciences and Engineering, 17 (3) (2020): 1973-2002.

[19] S. Bentout, S. Djilali, T. M. Touaoula, A. Zeb, A. Atangana, Bifurcation analysis for a double age dependence epidemic model with two delays, Nonlinear Dynamics, 108 (2022): 1821-1835.

[20] R. Z. Yang, D. Jin, W. L. Wang, A diffusive predator-prey model with generalist predator and time delay, AIMS Mathematics, 7 (3) (2022): 4574-4591.

[21] S. Li, C. D. Huang, S. L. Yuan, Hopf bifurcation of a fractional-order double-ring structured neural network model with multiple communication delays, Nonlinear Dynamics, 108 (2022): 379-396.

[22] C. J. Xu, M. X. Liao, P. L. Li, Bifurcation control for a fractional-order competition modelof Internet with delays, Nonlinear Dynamics, 95 (4) (2019): 3335-3356.

[23] H. F. Huo, Y. L. Chen, H. Xiang, Stability of a binge drinking model with delay, Journal of Biological Dynamics, 11(2017): 210-225.

[24] X. D. Yu, A. Y. Wan, Dynamical aspects of a delayed SEI2RS malware dissemination model in cyber-physical systems, Results in Physics, 40(2022): 1-10.

[25] C. X. Sun, J. W. Jia, Optimal control of a delayed smoking model with immigration, Journal of Biological Dynamics, 13(2019):447-460.

[26] C. R. Li, Z. J. Ma, Dynamics analysis and optimal control for a delayed rumor-spreading model, Mathematics, 10(2022):1-25.

[27] B. D. Hassard, N. D. Kazarinoff, Y. H. Wan, Theory and Applications of Hopf Bifurcation, Cambridge University Press, Cambridge 1981.

[28] C. R. Li, A study on time-delay rumor propagation model with saturated control function, Advances in Difference Equations, 255(2017):1-22.

[29] R. K. Upadhyay, S. Kumari, Discrete and data packet delays as determinants of switching stability in wireless sensor networks, Applied Mathematical Modelling, 72(2019):513-536.